Feedback Cooling of an Atomic Spin Ensemble

N. Behbood,[1] G. Colangelo,[1] F. Martin Ciurana,[1] M. Napolitano,[1] R. J. Sewell,[1] and M. W. Mitchell[1,2]
[1]*ICFO-Institut de Ciencies Fotoniques, Mediterranean Technology Park, 08860 Castelldefels (Barcelona), Spain*
[2]*ICREA-Institució Catalana de Recerca i Estudis Avançats, 08015 Barcelona, Spain*
(Received 24 May 2013; published 3 September 2013)

We apply entropy removal by measurement and feedback to a cold atomic spin ensemble. Using quantum nondemolition probing by Faraday rotation measurement, and feedback by weak optical pumping, we drive the initially random collective spin variable $\hat{\mathbf{F}}$ toward the origin $\hat{\mathbf{F}} = \mathbf{0}$. We use input-output relations and ensemble quantum noise models to describe this quantum control process and identify an optimal two-round control procedure. We observe 12 dB of spin noise reduction, or a factor-of-63 reduction in phase-space volume. The method offers a nonthermal route to generation of exotic entangled states in ultracold gases, including macroscopic singlet states and strongly correlated states of quantum lattice gases.

DOI: 10.1103/PhysRevLett.111.103601 PACS numbers: 42.50.Gy, 37.10.De, 37.10.Gh

Many physical phenomena are accessible only at low temperatures, with examples ranging from superfluidity [1,2] and the fractional quantum Hall effect [3] to quantum computing [4,5], quantum-enhanced sensing [6–9], and quantum simulation [10–12]. Traditional cooling couples the system of interest to a cold reservoir, allowing energy and entropy to leave the system. In contrast, feedback cooling [13] is a nonthermal process employing nondestructive measurement and feedback to remove entropy. This circumvents the requirements for a cold reservoir and for thermalization, which can be limiting in systems with finite lifetimes, e.g., atomic quantum simulators [14].

Feedback cooling has been applied to particle beams [13], trapped electrons [15], nanomechanical resonators [16,17], single ions [18], single atoms [19], dielectric microspheres [20,21], and quantum fields in cavity QED [22,23]. In addition to preparing a low-entropy state, feedback cooling on a many-body system has the potential to generate large-scale entanglement. For example, recent proposals for employing quantum nondemolition (QND) measurement of spin ensembles describe the generation of macroscopic singlet states [24,25], and also structured quantum correlations [26,27] characteristic of high-temperature superconductors [28]. Quantum correlations in the measurement-feedback process can be described by quantum control theory [29,30].

Here we experimentally demonstrate feedback cooling of the collective spin $\hat{\mathbf{F}}$ of an ^{87}Rb atomic ensemble using QND measurement [31–33] by near-resonant Faraday rotation measurement and feedback by weak optical pumping. Starting from a high-entropy state, i.e., a distribution occupying a large volume of collective spin phase space, measurement plus feedback moves the system toward $|\hat{\mathbf{F}}|^2 = \mathbf{0}$, which has zero phase-space volume. We analyze this quantum control problem using input-output relations and ensemble-based noise models [34,35], to identify an optimal two-round feedback protocol. Applying this strategy we observe spin noise reduction by 12 dB and phase-space volume reduction by a factor of 63, in good agreement with theory.

System.—The experiment is shown schematically in Fig. 1(a). Our atomic spin ensemble consists of $N_A \approx 10^6$ rubidium-87 atoms in the $f = 1$ ground hyperfine level, held in an optical dipole trap elongated in the z direction. The optical dipole trap is realized by a 7 W, linearly polarized, continuous-wave beam from a 1064 nm fiber laser focused to a waist of 50 μm. The size of the atomic cloud is 8.5 mm $\times$ 20 μm (FWHM). The measured trap lifetime is 30 s [36]. Interactions among the atoms due to collisions and magnetic dipolar couplings are negligible at our density of $\sim 10^{11}$ cm^{-3}.

We define the collective spin operator $\hat{\mathbf{F}} \equiv \sum_i \hat{\mathbf{f}}^{(i)}$, where $\hat{\mathbf{f}}^{(i)}$ is the spin of the ith atom. The collective spin obeys commutation relations $[F_x, F_y] = iF_z$ (we take $\hbar = 1$ throughout). Probe pulses are described by the Stokes operator $\hat{\mathbf{S}}$ defined as $\hat{S}_i \equiv 1/2(\hat{a}_+^\dagger, \hat{a}_-^\dagger)\sigma_i(\hat{a}_+, \hat{a}_-)^T$, where the σ_i are the Pauli matrices and $\hat{a}_\pm$ are annihilation operators for $\sigma_\pm$ polarization. As with $\hat{\mathbf{F}}$, the components of $\hat{\mathbf{S}}$ obey $[\hat{S}_x, \hat{S}_y] = i\hat{S}_z$ and cyclic permutations. The input pulses are fully $\hat{S}_x$ polarized, i.e., with $\langle \hat{S}_x \rangle = N_L/2$, $\langle \hat{S}_y \rangle = \langle \hat{S}_z \rangle = 0$, and $\Delta^2 S_i = N_L/4$, $i \in \{x, y, z\}$, where N_L is the number of photons in the pulse. While passing through the ensemble, the probe pulses experience the interaction Hamiltonian $\hat{H}_{\text{eff}} = \kappa_1 \tau^{-1} \hat{S}_z \hat{F}_z$, where κ_1 is a coupling coefficient for vector light shifts [35,37]. This rotates the pulse by an angle $\phi = \kappa_1 \hat{F}_z \ll 1$, so that a measurement of $\hat{S}_y^{(\text{out})}/\hat{S}_x^{(\text{in})}$ indicates $\hat{F}_z$ with a shot-noise-limited sensitivity of $\Delta \hat{F}_z = \Delta \hat{S}_y/\kappa_1$. Tensor light shifts are negligible in this work [32].

Control strategy.—Our aim is to reduce the state's phase-space volume $\Delta^2 \hat{\mathbf{F}} \equiv \langle |\hat{\mathbf{F}}|^2 \rangle - |\langle \hat{\mathbf{F}} \rangle|^2$ using measurement and feedback to sequentially set $\hat{F}_z$, $\hat{F}_y$, and $\hat{F}_x$ to desired values. In this experiment, the desired values are zero mean

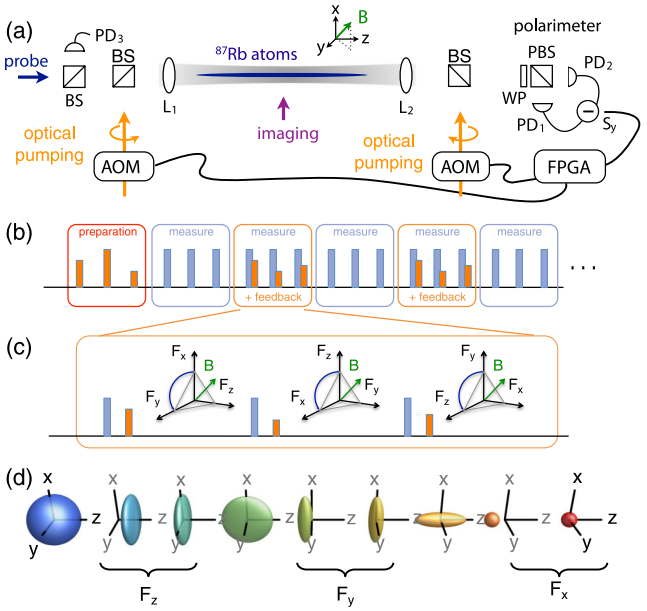

FIG. 1 (color online). Experimental schematic, pulse sequence, and control diagram for spin cooling by QND measurement plus feedback. (a) Experimental geometry. Near-resonant probe pulses pass through a cold cloud of ^{87}Rb atoms and experience a Faraday rotation by an angle proportional to the on-axis collective spin $\hat{F}_z$. The pulses are initially polarized with maximal Stokes operator $\hat{S}_x$ recorded on reference detector (PD_3). Rotation toward $\hat{S}_y$ is detected by a balanced polarimeter consisting of a wave plate (WP), polarizing beam splitter (PBS), and photodiodes ($PD_{1,2}$). A field-programable gate array (FPGA)-based controller interprets the polarimeter signal and reference and produces optical feedback pulses via acousto-optic modulators (AOMs). $\hat{\mathbf{F}}$ precesses about a magnetic field ($\mathbf{B}$) along the direction [111] making all components accessible to measurement and feedback through stroboscopic probing. (b), (c) Pulse sequence: A first QND measurement measures the $\hat{F}_z$ angular momentum component and the FPGA calculates the Faraday rotation angle in ≈ 11 μs. The FPGA applies a control pulse, proportional to the Faraday rotation angle, to an AOM to generate optical-pumping feedback. At the appropriate times in the Faraday rotation cycle, the same process is applied also to $\hat{F}_y$ and $\hat{F}_x$. (d) Evolution of the state in $\hat{\mathbf{F}}$ phase space as it is transformed by successive measurement, feedback, and precession steps.

value for all components of angular momentum. This is possible using QND measurements and nondestructive feedback, which we implement with weak optical pumping. The spin uncertainty relations, $\Delta\hat{F}_i\Delta\hat{F}_j \geq |\langle\hat{F}_k\rangle|/2$, even allow $\Delta^2\hat{\mathbf{F}}$ to approach zero for the macroscopic singlet state [24]. Faraday rotation gives high-sensitivity measurement of $\hat{F}_z$. To access $\hat{F}_x$ and $\hat{F}_y$, we apply a static magnetic field of $B \approx 14$ mG along the [111] axis (Larmor period $T_L \simeq 120$ μs) to induce $\hat{F}_z \to \hat{F}_x \to \hat{F}_y$ precession, and probe at $T_L/3$ intervals. The optical pumping performs a controlled displacement of the spin state (a rotation would leave $|\hat{\mathbf{F}}|$ unchanged) toward a desired value. As described below, multi-round feedback is expected to give additional cooling. For this reason we repeat the three-axis measurement and feedback. The experimental sequence is illustrated in Fig. 1(b).

QND measurement.—We measure the collective spin component $\hat{F}_z$ by paramagnetic Faraday rotation probing with 1 μs long pulses of linearly polarized light with on average $N_L = 5.4 \times 10^7$ photons per pulse at a detuning of 700 MHz to the red of the $f = 1 \to f' = 0$ transition. Measurements are made at $T_L/3 \simeq 40$ μs intervals, to access sequentially $\hat{F}_z$, $\hat{F}_y$, and $\hat{F}_x$. A shot-noise-limited balanced polarimeter detects $\hat{S}_y^{(\mathrm{out})}$ while a reference detector before the atoms measures $\hat{S}_x^{(\mathrm{in})}$ [31]. Both signals are collected by a real-time field-programable gate array (FPGA)-based controller, which computes the measurement result $\mathcal{F} \equiv \hat{S}_y^{(\mathrm{out})}/(\kappa_1\hat{S}_x^{(\mathrm{in})})$ and generates timing signals to control the optical pumping feedback.

Optical pumping and feedback.—The optical pumping is performed in a nearly linear regime, i.e., with few photons, such that only a small fraction of the atoms changes state. We use circularly polarized light 30 MHz red detuned from the $f = 1 \to f' = 0$ transition on the D_2 line with an intensity ~ 7 W/m^2, propagating along the trap axis and chopped into $\sim\mu$s pulses by acousto-optic modulators (AOMs). This detuning reduces shadowing effects and gives more uniform optical pumping, while still being significantly closer to the closed $F = 1 \to F' = 0$ transition than to other $F = 1 \to F'$ transitions, reducing optical pumping of atoms into the $F = 2$ ground state. Two beams in opposite directions allow rapid switching between the two circular polarizations. As with the QND measurement, Larmor precession allows feedback to $\hat{F}_z$, $\hat{F}_y$, and $\hat{F}_x$ by $\hat{F}_z$ pumping at different points in the cycle. In the feedback step the AOMs are gated by the FPGA after a latency of $t_{\mathrm{lat}} = 11$ μs for computation. The FPGA determines the polarization and pulse duration $t_{\mathrm{FB}} \propto \mathcal{F}$, which in turn determines the displacement of $\hat{\mathbf{F}}$. Typical feedback pulses are 1–2 μs, i.e., much shorter than the Larmor precession period, and much longer than the $\sim$100 ns rise time of the AOMs. An independent AOM amplitude control determines the overall gain of the feedback.

Initialization procedure.—We first generate a fully mixed $f = 1$ state as described in [31], apply the magnetic field along the [111] direction, then sequentially optically pump $\hat{F}_z$, $\hat{F}_y$, and $\hat{F}_x$ with 5 μs pulses. The amplitude A and polarization sign s of the pulses are randomly chosen so that sA is zero-mean normally distributed. This generates a statistically reproducible distribution of initial states with initial spin covariance matrix $\Gamma_F \equiv (1/2) \times \langle\hat{F}_i\hat{F}_j + \hat{F}_j\hat{F}_i\rangle - \langle\hat{F}_i\rangle\langle\hat{F}_j\rangle$ of

$$\Gamma_F = \begin{pmatrix} 2.70 & -0.03 & -1.20 \\ -0.03 & 2.30 & -0.65 \\ -1.20 & -0.65 & 2.20 \end{pmatrix} \times 10^8 \text{ spins}^2, \quad (1)$$

i.e., with noises $N_A^{1/2} \ll \Delta\hat{F}_i \ll N_A \simeq 10^6$.

Control and characterization sequence.—For a given normalized gain $g \equiv G/G_0$, where G is the feedback gain and G_0 is the naive gain, i.e., optimal gain for the noiseless case, we characterize the cooling process with the sequence shown in Fig. 1(b): initial state preparation, measurement without feedback, measurement with feedback, and measurement without feedback. We then remove the atoms from the trap and repeat the same sequence to record the measurement readout noise. The entire cycle is run 300 times to collect statistics.

In Fig. 2(a) we plot the input spin distribution (blue) following our initialization procedure, and the output spin distribution (red) after feedback with the optimum feedback gain setting. The input state is distributed around the origin, with a mean deviation of 2.4×10^4 spins and a total variation of $\Delta^2\hat{\mathbf{F}} = 6.7 \times 10^8$ spins^2. Histograms of the measurements are shown in Figs. 2(b)–2(d). After feedback (red data) the total variation of the spin distribution is $\Delta^2\hat{\mathbf{F}} = 9.7 \times 10^7$ spins^2, an 8 dB reduction in a single feedback step. The dispersion of all three spin components is reduced by a factor of 3–5, and the average of each spin component remains centered within 1 standard deviation of the origin.

Correlations analysis.—Covariance matrices describing all nine measurements, for $g = 0$ (null case) and gains $g = -0.75$ (optimal case). are shown in Fig. 3. Three features are noteworthy. (1) Both null and optimal cases show strong correlations between the first and second measurement groups, confirming the nondestructive nature of the Faraday rotation measurement. (2) The correlations of one component, e.g., $\hat{F}_y$, persist even after feedback to another component, e.g., $\hat{F}_z$, indicating the nondestructive nature of the optical feedback. (3) While the control case shows some reduction of total variance (due to spin relaxation), the feedback control is far more effective.

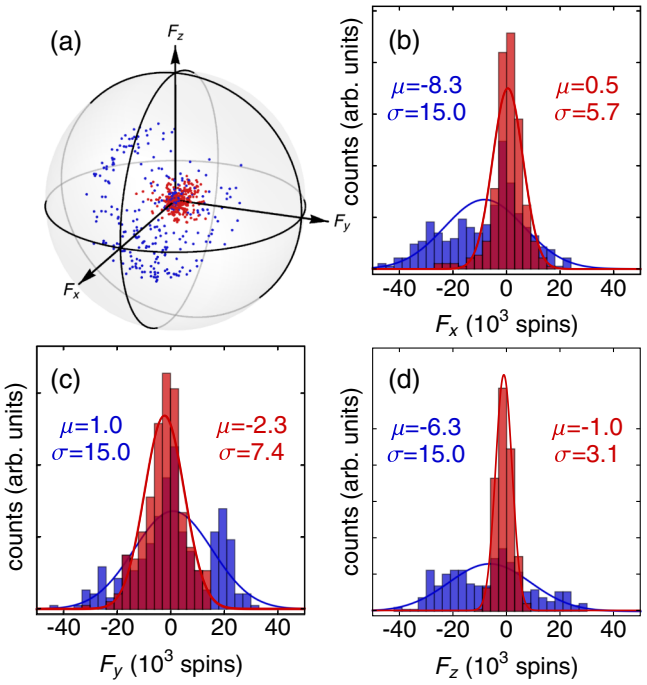

FIG. 2 (color online). Input and output spin distributions. (a) Measured input spin distribution (blue data) following the initialization procedure described in the main text, and measured output spin distribution (red data) following a single feedback step with the optimum feedback gain setting. The gray sphere has a radius of 6×10^4 spins. (b)–(d) Histograms of the measurements of each of the three spin components before (blue) and after (red) feedback. See text for details.

Modeling.—We use a multistep input-output model of the collective spin operators to describe the feedback cooling process. During a step of length Δt, an operator $\hat{O}$ experiences $\hat{O}^{(i+1)} = \hat{O}^{(i)} - i\Delta t[\hat{O}^{(i)}, \hat{H}^{(i)}_{\text{eff}}] + \mathcal{N}$, where superscripts (i), $(i+1)$ indicate prior and posterior values, respectively, and $\mathcal{N}$ is a noise operator. Starting from atomic and optical inputs $\hat{\mathbf{F}}^{(0)}$, $\hat{\mathbf{S}}^{(0)}$, respectively, a Faraday rotation measurement produces

$$\hat{S}_y^{(1)} = \hat{S}_y^{(0)} + \kappa_1 \hat{S}_x^{(\text{in})} \hat{F}_z^{(0)}, \tag{2}$$

$$\hat{\mathbf{F}}^{(1)} = (1-\eta)\hat{\mathbf{F}}^{(0)} - i\tau[\hat{\mathbf{F}}^{(0)}, \hat{F}_z]\hat{S}_z^{(0)} + \hat{\mathbf{N}}^{(S)}, \tag{3}$$

with $\hat{S}_x$, $\hat{S}_z$ changing negligibly. Measurement backaction on the atoms $-i\tau[\hat{\mathbf{F}}^{(0)}, \hat{F}_z]\hat{S}_z^{(0)}$ is small provided $|\langle \hat{F}_x \rangle|$, $|\langle \hat{F}_y \rangle| \ll N_A$. $\hat{\mathbf{N}}^{(S)}$ arises from the fraction η of atoms that suffer spontaneous emission (see below). During latency, precession by an angle $\theta = 2\pi t_{\text{lat}}/T_L$ about [111] causes coherent rotation $R_{\mathbf{B}}(\theta)$ and dephasing due to field inhomogeneities [35,38]:

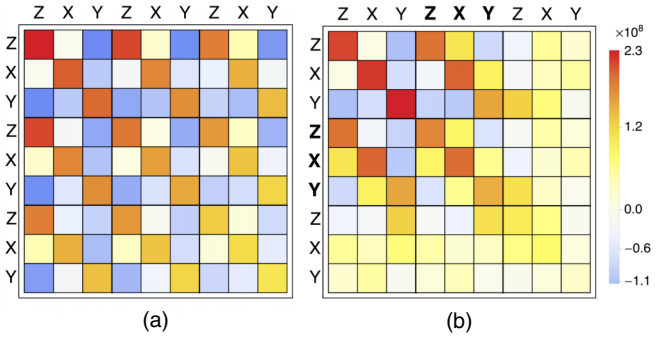

FIG. 3 (color online). Correlation between consecutive three-component collective spin measurements. (a) Covariance matrix for 9 consecutive stroboscopic measurements with no feedback showing strong correlations between all three measurements of each spin component $\hat{F}_i$ (red and orange squares). (b) Covariance matrix for 9 consecutive stroboscopic measurements with feedback after measurements 4–6 (indicated in bold font) with the optimal gain setting. The first two measurements of each spin component $\hat{F}_i$ remain strongly correlated, but the correlation is removed by the feedback and the third set of measurements is not correlated with the first two. Also apparent is the noise reduction after feedback. The anticorrelation of $\hat{F}_z$ and $\hat{F}_y$ reflects the nonisotropic noise of the initial state, which is visible in Fig. 2(a).

$$\hat{\mathbf{F}}^{(2)} = X(\theta)\hat{\mathbf{F}}^{(1)} + \hat{\mathbf{N}}^{(\theta)}, \tag{4}$$

$$X(\theta) \equiv P_{\mathbf{B}} + \exp\left[-\frac{\theta}{\omega_L T_2}\right] R_{\mathbf{B}}(\theta)(\mathbb{1} - P_{\mathbf{B}}), \tag{5}$$

where $P_{\mathbf{B}}$ is a projector onto the [111] direction and T_2 is the transverse relaxation time. Longitudinal relaxation is negligible on the time scale of the experiment. Feedback modifies the collective spin as

$$\hat{\mathbf{F}}^{(3)} = G\mathbb{F}_z\hat{S}_y^{(2)} + \hat{\mathbf{F}}^{(2)} + \hat{\mathbf{N}}^{(\mathrm{FB})}, \tag{6}$$

where G is the feedback gain and $\mathbb{F}_z$ is a unit vector in the z direction. Precession by $\bar{\theta} = 2\pi/3 - \theta$ completes the $1/3$ Larmor rotation, giving

$$\hat{\mathbf{F}}^{(4)} = X(\bar{\theta})[G\mathbb{F}_z(\hat{S}_y^{(0)} + \kappa_1\hat{S}_x\hat{F}_z^{(0)}) + X(\theta)\hat{\mathbf{F}}^{(0)} + \hat{\mathbf{N}}^{(\mathrm{FB})} + \hat{\mathbf{N}}^{(\theta)} + \hat{\mathbf{N}}^{(S)}] + \hat{\mathbf{N}}^{(\bar{\theta})} \tag{7}$$

for measurement plus feedback for one component.

The vector feedback procedure is the composition of three transformations as in Eq. (7). These correct sequentially for all three components of $\hat{\mathbf{F}}$, and introduce a total of twelve noise terms analogous to $\hat{S}_y^{(0)}$, $\hat{\mathbf{N}}^{(\mathrm{FB})}$, $\hat{\mathbf{N}}^{(\theta)}$, and $\hat{\mathbf{N}}^{(\bar{\theta})}$, given in the Appendix.

Optimized multistep cooling.—We define the normalized gain $g \equiv G/|G_0|$, where $G_0 \equiv -1/(\kappa_1\hat{S}_x)$ is the naive gain, i.e., the optimal gain for when noise, dephasing, and latency are zero. Minimizing $\Delta^2\hat{\mathbf{F}}^{(4)}$ requires $-1 < g < 0$ because of competition between the $G\mathbb{F}_z\hat{S}_y^{(0)}$ and $G\mathbb{F}_z\kappa_1\hat{S}_x\hat{F}_z^{(0)} - X(\theta)\hat{\mathbf{F}}^{(0)}$ contributions in Eq. (7). Moreover, the optimal g increases with increasing signal-to-noise ratio $\Delta^2\hat{\mathbf{F}}^{(0)}/\Delta^2\hat{S}_y^{(0)}$. This suggests a multiround feedback strategy employing successive three-axis feedback steps, with decreasing $|g|$, to approach the limiting entropy set by $\Delta^2\hat{S}_y^{(0)}$ and $\Delta^2\hat{\mathbf{N}}^{(S)}$.

We demonstrate this optimized multistep cooling with results shown in Fig. 4. Again following the sequence of Fig. 1, we initialize to give measured total spin variance $\Delta^2\hat{\mathbf{F}} \approx 6.7 \times 10^8$ spins^2, shown as blue circles. In a first experiment we apply a single round of three-axis measurement plus feedback, then measure the resulting state, and compute total variance (red triangles). As expected, an optimum is observed at $g \simeq -0.75$, with variance 9.7×10^7 spins^2 or 8 dB reduction in the spin noise. In a second experiment we apply a first round with $g = -0.75$ followed by a second round with variable g, shown as green diamonds. This gives an additional 4 dB reduction, to 4.2×10^7 spins^2. Further cooling should be possible with additional feedback steps, and was limited in this experiment by the resolution of the optical pumping feedback mechanism. Model predictions, with $\kappa_1 = 1.1 \times 10^{-7}$, $N_A = 10^6$, $N_L = 5.4 \times 10^7$, $T_2 = 1.3$ ms from independent measurements, are fit to the global data set to calibrate the optical pumping efficiency (effectively g) and the initial noise $\Delta^2\hat{\mathbf{F}}^{(0)}$. Good agreement is observed except for $g \leq -1.25$. The discrepancy is possibly due to saturation of the optical pumping, which we have seen for shifts $\delta F_z \approx 3.5 \times 10^4$ spins, comparable to the largest initial spin values. For $|g| > 1$, saturation would reduce the effective gain, consistent with Fig. 4.

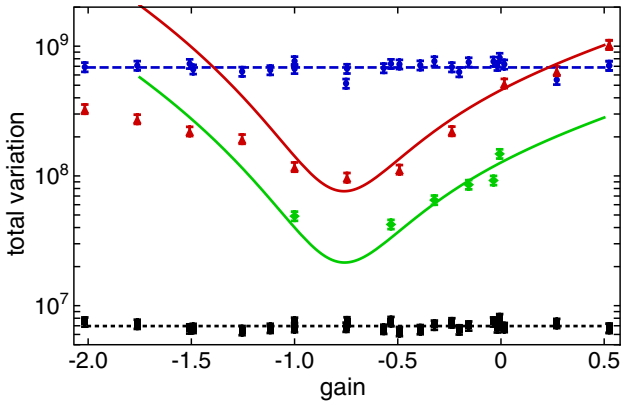

FIG. 4 (color online). Spin cooling via optical feedback. Measured total variation $\Delta^2\hat{\mathbf{F}}$ following one (red triangles) and two (green diamonds) feedback steps. We compare this to the theory described in the text (red and green solid curves) fit to the $g \geq -1.0$ data. Also shown is the noise of the input spin state following the initialization procedure (blue circles), with an average total variation $\Delta^2\hat{\mathbf{F}} = 6.7 \times 10^8$ spins^2 (blue dashed line), and the measurement readout noise (black squares), with an average total variation $\Delta^2\hat{\mathbf{F}} = 7.0 \times 10^6$ spins^2 (black dotted line). Error bars represent $\pm 1\sigma$ statistical errors.

Conclusion.—Using Faraday rotation quantum nondemolition measurements and feedback by optical pumping, we have reduced the spin variance of a laser-cooled ^{87}Rb atomic ensemble. The total spin variance $\Delta^2\hat{\mathbf{F}}$ is reduced by 12 dB, or a reduction in phase-space volume by a factor of 63, using an optimized two-step procedure informed by a realistic quantum control theory incorporating experimental imperfections. The procedure has potential application to on-demand generation of quantum-correlated states of ultracold atomic gases, for example, generation of macroscopic singlet states and arbitrary quantum correlations in lattice-bound degenerate quantum gases.

We thank B. Dubost and G. Tóth for helpful discussions. This work was supported by the Spanish MINECO under the project MAGO (Reference No. FIS2011-23520), by the European Research Council under the project AQUMET, and by Fundació Privada CELLEX.

Appendix: Noise terms.—Readout noise is $\Delta^2\hat{S}_y^{(0)} = N_L/4$, as above. $\hat{\mathbf{N}}^{(S)}$ arises from spontaneous emission events, which randomize the spins of a fraction $\eta_S \approx 2\kappa_1^2 N_A N_L/(3\alpha_0)$ of the atoms [34,39], introducing a noise $\Delta^2 N_i^{(S)} = \Delta^2 f_i^{(1)}\eta_S(1-\eta_S)N_A + \eta_S N_A f(f+1)/3$, where $\hat{\mathbf{f}}_i^{(1)}$ is the mean single-atom spin vector. For unpolarized states, $\Delta^2 N_i^{(S)} \approx N_A\eta_S(2-\eta_S)f(f+1)/3$. Similarly, dephasing randomizes the transverse polarizations of a

fraction $\eta_D \equiv 1 - \exp[\theta/(2\pi T_L)]$ giving noise $\Delta^2 N_i^{(\theta)} \approx N_A \eta_D (2 - \eta_D) f(f+1)/3$. The optical pumping process is stochastic but uncorrelated among the atoms, leading to a multinomial distribution in the displacement $\hat{\mathbf{F}}^{(\mathrm{FB})} \equiv \hat{\mathbf{F}}^{(2)} - \hat{\mathbf{F}}^{(1)}$ and a noise $\hat{\mathbf{N}}^{(\mathrm{FB})} \propto |\langle \hat{\mathbf{F}}^{(\mathrm{FB})} \rangle|^{1/2}$, which is $\ll |\langle \hat{\mathbf{F}}^{(\mathrm{FB})} \rangle|$ except if $|\langle \hat{\mathbf{F}}^{(\mathrm{FB})} \rangle| \sim 1$. In this experiment with large α_0 and small N_L, only $\hat{S}_y^{(0)}$ and $\hat{\mathbf{N}}^{(S)}$ make a significant contribution.

[1] E. F. Burton, Nature (London) **135**, 265 (1935).
[2] P. Kapitza, Nature (London) **141**, 74 (1938).
[3] D. C. Tsui, H. L. Stormer, and A. C. Gossard, Phys. Rev. Lett. **48**, 1559 (1982).
[4] J. Chiaverini, J. Britton, D. Leibfried, E. Knill, M. D. Barrett, R. B. Blakestad, W. M. Itano, J. D. Jost, C. Langer, R. Ozeri, T. Schaetz, and D. J. Wineland, Science **308**, 997 (2005).
[5] T. Monz, K. Kim, A. S. Villar, P. Schindler, M. Chwalla, M. Riebe, C. F. Roos, H. Häffner, W. Hänsel, M. Hennrich, and R. Blatt, Phys. Rev. Lett. **103**, 200503 (2009).
[6] J. Appel, P. J. Windpassinger, D. Oblak, U. B. Hoff, N. Kjærgaard, and E. S. Polzik, Proc. Natl. Acad. Sci. U.S.A. **106**, 10 960 (2009).
[7] M. H. Schleier-Smith, I. D. Leroux, and V. Vuletić, Phys. Rev. Lett. **104**, 073604 (2010).
[8] C. Gross, T. Zibold, E. Nicklas, J. Esteve, and M. K. Oberthaler, Nature (London) **464**, 1165 (2010).
[9] R. J. Sewell, M. Koschorreck, M. Napolitano, B. Dubost, N. Behbood, and M. W. Mitchell, Phys. Rev. Lett. **109**, 253605 (2012).
[10] S. Lloyd, Science **273**, 1073 (1996).
[11] E. Jané, G. Vidal, W. Dür, P. Zoller, and J. I. Cirac, Quantum Inf. Comput. **3**, 15 (2003).
[12] M. Lewenstein, A. Sanpera, and V. Ahufinger, *Ultracold Atoms in Optical Lattices: Simulating Quantum Many-Body Systems* (Oxford University Press, Oxford, England, 2012).
[13] S. van der Meer, Rev. Mod. Phys. **57**, 689 (1985).
[14] S. Trotzky, Y.-A. Chen, A. Flesch, I. P. McCulloch, U. Schollwock, J. Eisert, and I. Bloch, Nat. Phys. **8**, 325 (2012).
[15] B. D'Urso, B. Odom, and G. Gabrielse, Phys. Rev. Lett. **90**, 043001 (2003).
[16] A. Hopkins, K. Jacobs, S. Habib, and K. Schwab, Phys. Rev. B **68**, 235328 (2003).
[17] M. Poggio, C. L. Degen, H. J. Mamin, and D. Rugar, Phys. Rev. Lett. **99**, 017201 (2007).
[18] P. Bushev, D. Rotter, A. Wilson, F. Dubin, C. Becher, J. Eschner, R. Blatt, V. Steixner, P. Rabl, and P. Zoller, Phys. Rev. Lett. **96**, 043003 (2006).
[19] M. Koch, C. Sames, A. Kubanek, M. Apel, M. Balbach, A. Ourjoumtsev, P. W. H. Pinkse, and G. Rempe, Phys. Rev. Lett. **105**, 173003 (2010).
[20] T. Li, S. Kheifets, and M. G. Raizen, Nat. Phys. **7**, 527 (2011).
[21] J. Gieseler, B. Deutsch, R. Quidant, and L. Novotny, Phys. Rev. Lett. **109**, 103603 (2012).
[22] C. Sayrin, I. Dotsenko, X. Zhou, B. Peaudecerf, T. Rybarczyk, S. Gleyzes, P. Rouchon, M. Mirrahimi, H. Amini, M. Brune, J.-M. Raimond, and S. Haroche, Nature (London) **477**, 73 (2011).
[23] X. Zhou, I. Dotsenko, B. Peaudecerf, T. Rybarczyk, C. Sayrin, S. Gleyzes, J. M. Raimond, M. Brune, and S. Haroche, Phys. Rev. Lett. **108**, 243602 (2012).
[24] G. Tóth and M. W. Mitchell, New J. Phys. **12**, 053007 (2010).
[25] I. Urizar-Lanz, P. Hyllus, I. Egusquiza, M. W. Mitchell, and G. Toth, Phys. Rev. A **88**, 013626 (2013).
[26] P. Hauke, R. J. Sewell, M. W. Mitchell, and M. Lewenstein, Phys. Rev. A **87**, 021601 (2013).
[27] K. Eckert, O. Romero-Isart, M. Rodriguez, M. Lewenstein, E. S. Polzik, and A. Sanpera, Nat. Phys. **4**, 50 (2008).
[28] P. W. Anderson, Science **235**, 1196 (1987).
[29] H. Mabuchi and N. Khaneja, Int. J. Robust Nonlinear Control **15**, 647 (2005).
[30] S. Chaudhury, S. Merkel, T. Herr, A. Silberfarb, I. H. Deutsch, and P. S. Jessen, Phys. Rev. Lett. **99**, 163002 (2007).
[31] M. Koschorreck, M. Napolitano, B. Dubost, and M. W. Mitchell, Phys. Rev. Lett. **104**, 093602 (2010).
[32] M. Koschorreck, M. Napolitano, B. Dubost, and M. W. Mitchell, Phys. Rev. Lett. **105**, 093602 (2010).
[33] R. J. Sewell, M. Napolitano, N. Behbood, G. Colangelo, and M. W. Mitchell, Nat. Photonics **7**, 517 (2013).
[34] M. Koschorreck and M. W. Mitchell, J. Phys. B **42**, 195502 (2009).
[35] G. Colangelo, R. J. Sewell, N. Behbood, F. M. Ciurana, and M. W. Mitchell, arXiv:1305.0444.
[36] M. Kubasik, M. Koschorreck, M. Napolitano, S. R. de Echaniz, H. Crepaz, J. Eschner, E. S. Polzik, and M. W. Mitchell, Phys. Rev. A **79**, 043815 (2009).
[37] S. R. de Echaniz, M. Koschorreck, M. Napolitano, M. Kubasik, and M. W. Mitchell, Phys. Rev. A **77**, 032316 (2008).
[38] N. Behbood, F. M. Ciurana, G. Colangelo, M. Napolitano, M. W. Mitchell, and R. J. Sewell, Appl. Phys. Lett. **102**, 173504 (2013).
[39] L. B. Madsen and K. Mølmer, Phys. Rev. A **70**, 052324 (2004).